

# Structural determinants of ligand migration in *Mycobacterium tuberculosis* truncated hemoglobin O

Leonardo Boechi,<sup>1</sup> Marcelo A. Martí,<sup>1</sup> Mario Milani,<sup>2</sup> Martino Bolognesi,<sup>2</sup> F. Javier Luque,<sup>3</sup> and Darío A. Estrin<sup>1\*</sup>

<sup>1</sup>Departamento de Química Inorgánica, Analítica y Química Física/INQUIMAE-CONICET, Facultad de Ciencias Exactas y Naturales, Universidad de Buenos Aires, Ciudad Universitaria, Pabellón II, Buenos Aires, Argentina

<sup>2</sup>Department of Biomolecular Sciences and Biotechnology and CNR-INFM, University of Milano, Milano, Italy

<sup>3</sup>Departament de Físicoquímica and Institut de Biomedicina, Facultat de Farmàcia, Universitat de Barcelona, Avenida Diagonal, Barcelona, Spain

## ABSTRACT

*Mycobacterium tuberculosis* is the causative agent of human tuberculosis, one of the most prevalent infectious diseases in the world. Its genome hosts the *glbN* and *glbO* genes coding for two proteins, truncated hemoglobin N (trHbN) and truncated hemoglobin O (trHbO), that belong to different groups (I and II, respectively) of the recently discovered trHb family of heme proteins. The different expression pattern and kinetics rates constants for ligand association and NO oxidation rate suggest different functions for these proteins. Previous experimental and theoretical studies showed that, in trHbs, ligand migration along the internal tunnel cavity system is a key issue in determining the ligand-binding characteristics. The X-ray structure of trHbO has been solved and shows several internal cavities and secondary-docking sites. In this work, we present an extensive investigation of the tunnel/cavity system of *M. tuberculosis* trHbO by means of computer-simulation techniques. We have computed the free-energy profiles for ligand migration along three found tunnels in the oxy and deoxy w.t. and mutant trHbO proteins. Our results show that multiple-ligand migration paths are possible and that several conserved residues such as TrpG8 play a key role in the ligand-migration regulation.

Proteins 2008; 73:372–379.  
© 2008 Wiley-Liss, Inc.

**Key words:** truncated hemoglobin; *Mycobacterium tuberculosis*; molecular dynamics; ligand migration; jarzynski.

## INTRODUCTION

*Mycobacterium tuberculosis* is the causative agent of human tuberculosis, one of the most prevalent infectious diseases in the world.<sup>1,2</sup> According to the World Health Organization, tuberculosis affects approximately two billion people world-wide, causing over three million deaths each year.<sup>3</sup> The genome of this pathogenic organism hosts the *glbN* and *glbO* genes coding for two proteins, truncated hemoglobin N (trHbN) and truncated hemoglobin O (trHbO), that belong to a recently discovered family of heme proteins, widely distributed in eubacteria, cyanobacteria, protozoa, and plants.<sup>4</sup>

Members of the truncated hemoglobin family (trHbs) exhibit a three-dimensional structure related to the common globin fold of vertebrate globins but significantly simplified. In essence, trHbs consist of four  $\alpha$ -helices arranged in a two-over-two antiparallel sandwich that is a subset of the 3-on-3  $\alpha$ -helical sandwich fold characteristic of vertebrate globins.<sup>5–7</sup> The function of trHbs is poorly understood; roles such as O<sub>2</sub>/NO sensors, oxygen carriers under hypoxic conditions, or pseudoenzymes have been proposed.<sup>8–10</sup>

Phylogenetic and sequence analyses distinguished three different groups of truncated hemoglobins, which were denominated as trHbs groups I, II, and III. Some organisms such as *M. tuberculosis*, *M. avium*, and *M. smegmatis*, among others, display trHbs belonging to all three groups (alternatively labeled N, O, and, P for groups I, II, and III, respectively). It has been postulated that the genes corresponding to the same groups in different species are orthologs.<sup>11</sup> In general, trHbs of different groups in the same organism share about 20% sequence identity and the same

Additional Supporting Information may be found in the online version of this article.

Grant sponsors: Ministerio de Educación y Ciencia (grant CTQ2005-08797-C02-01). European Union FP7-HEALTH-2007-B Program (grant Nostress), FIRB grant “Biologia Strutturale” (Italian Ministry of University and Scientific Research), ANPCYT (National Science Agency of Argentina), CONICET, and University of Buenos Aires.

\*Correspondence to: Darío Estrin, Departamento de Química Inorgánica, Analítica y Química Física/INQUIMAE-CONICET, Facultad de Ciencias Exactas y Naturales, Universidad de Buenos Aires, Ciudad Universitaria, Pabellón II, Buenos Aires (C1428EHA), Argentina. E-mail: dario@qi.fcen.uba.ar

Received 19 November 2007; Revised 28 February 2008; Accepted 9 March 2008

Published online 23 April 2008 in Wiley InterScience (www.interscience.wiley.com).

DOI: 10.1002/prot.22072

group trHbs in different organisms share more than 80% identity. For example, *M. tuberculosis* trHbN and *M. tuberculosis* trHbO have a sequence identity of 18%, whereas *M. tuberculosis* trHbO and *M. avium* trHbO show sequence identity of 84%.<sup>8</sup>

Several microorganisms such as *Leishmania*, *Trypanosoma*, and *Plasmodium* are not able to withstand the high-NO concentrations produced by the macrophages upon infection. This is due to the fact that NO interferes with cysteine proteases, among other, that are vital for the microorganism's cell cycle.<sup>12,13</sup> Cell-culture studies have shown that *M. tuberculosis* hosts a molecular defense system responsible for NO resistance. It has been recently shown that trHbN is responsible for such NO protection mechanism<sup>8,14</sup> by means of a NO dioxygenase process, which leads to the release of nitrate. The trHbN dioxygenase mechanism would include a first step of O<sub>2</sub> binding, favored by the high O<sub>2</sub> affinity of the protein. Subsequently, NO would enter into the oxy-protein, migrate to the active site, and react with the coordinated oxygen to yield an unstable peroxynitrite adduct, whose isomerization would yield nitrate. Ligand (O<sub>2</sub> and NO) migration to the active site have been proposed to define the overall rate of the detoxification process.<sup>15</sup> Recent studies on trHbN suggested that a trHb group I specific tunnel/cavity system is subtly involved in ligand migration to/from the heme.<sup>14</sup>

Much less is known about the potential role of tunnels/cavities in the regulation of ligand migration in trHbO, thus in the modulation of group II trHb function. Experimental evidence indicates that O<sub>2</sub> binding to deoxy trHbO, and NO oxidation by oxy-trHbO, occur with similar rate constants, ( $1.1 \times 10^5$ – $8.5 \times 10^5$ ) M<sup>-1</sup> s<sup>-1</sup>, and ( $1.8 \times 10^5$ – $9.5 \times 10^5$ ) M<sup>-1</sup> s<sup>-1</sup>, respectively, suggesting that migration of both ligands to trHbO heme is limited by common (steric) restraints.<sup>16</sup>

In contrast to what is observed for trHbN, which is expressed during the stationary phase of the mycobacterium, trHbO is expressed during the whole cell cycle; in addition, kinetics rate constants for ligand association and NO oxidation are different for the two proteins.<sup>4</sup> Different functional roles have therefore been proposed for trHbO and trHbN. Some authors proposed that trHbO could be implicated in oxygen transport associated to the cell membrane.<sup>17,18</sup> However, this seems unlikely due to the low association rate between trHbO and O<sub>2</sub>. Recently, Ouellet *et al.*<sup>19</sup> have postulated that this protein has a peroxidatic activity. On the other hand, it has been demonstrated that trHbO from *M. leprae* (87.5% identity with trHbO from *M. tuberculosis*) is able to detoxify NO and alleviates the organism from nitric oxide toxicity.<sup>15</sup> Clearly, although much has been learned, the function and physiological relevance of *M. tuberculosis* trHbO, and of all other known trHbs from group II, is largely a matter of debate.

The X-ray structure of trHbO showed that the protein crystallized as a highly symmetrical dodecamer;<sup>20</sup> how-

ever, more recently, Pathania *et al.*<sup>17</sup> provided evidence supporting homodimeric structure in solution. An unusual covalent bridge linking the phenolic O atom of TyrB10 and the aromatic ring of TyrCD1 has been observed in 6 of the 12 subunits of the X-ray structure and confirmed by mass spectrometry of the protein in solution.<sup>20</sup> The physiological role of such intramolecular cross-bridge, unique within the hemoglobin superfamily, is totally unknown, as are its specific effects on ligand migration and binding.

In this work, we present an investigation of the tunnel/cavity system of trHbO by means of computer-simulation techniques. We performed simulations of the w.t. protein and of two heme distal site mutants, and we also analyzed the role of the TyrB10-TyrCD1 cross-bridge. Our goal is to shed light on the microscopic determinants that give rise to trHbO-specific functional properties, in the context of trHbs from different groups. We have paid special attention to the role of conserved residues in group II trHbs, and to residues, which may be relevant for the proposed reaction mechanisms. Because trHbs are found in diverse pathogenic organisms presenting high risks to human health, the ultimate goal of this study is a deeper understanding of how trHb structural determinants relate to their functions to cast ideas for the design of lead inhibitory compounds.

## METHODS

### Set up of the system

Molecular dynamics (MD) simulations were performed starting from the crystal structure of wild-type cyanomet trHbO, and solved at 2.1 Å resolution (PDB entry: 1NGK).<sup>20</sup> We have chosen as the starting structure the A subunit and replaced the CN<sup>-</sup> for an O<sub>2</sub> ligand. The system was immersed in a box of TIP3P<sup>21</sup> water molecules of about 60.0 × 50.0 × 70.0 Å. Water molecules located at less than 2.4 Å from any atom of the protein were removed. Seven Na<sup>+</sup> atoms were added to neutralize the system. The final system contains the protein, 7344 water molecules, and the added ions. All systems were simulated using periodic boundary conditions and Ewald sums for treating long-range electrostatic interactions. SHAKE<sup>22</sup> was used to keep bonds involving H atoms at their equilibrium length. This allowed us to use a 2-fs time step for the integration of Newton's equations. The parm99 and TIP3P force fields implemented in AMBER were used to describe the protein and water, respectively.<sup>23</sup> The oxygenated heme model system charges were determined using RESP charges and HF/6-31G(d) wave functions (see Supporting information). The temperature and pressure were regulated with the Berendsen thermostat and barostat, respectively, as implemented in AMBER.

All systems were equilibrated by first cooling slowly from 200 K to 0 K for 100 ps to optimize any possible structural clashes. Subsequently, the systems were heated slowly from 0 to 300 K for 200 ps under constant volume conditions. Finally, a short simulation at constant temperature of 300 K, under constant pressure of 1 bar, was performed for additional 500 ps to allow the systems to reach proper density. These equilibrated structures were the starting point for the production of MD simulations.

Mutations were performed *in silico* by changing the corresponding amino acid in the original structure and allowing the system to equilibrate as mentioned earlier. To build the covalent Tyr—Tyr bond, the phenolic hydrogen of TyrB10 (HH) and the HE2 of TyrCD1 hydrogen were removed, and a bond between TyrB10-OH and TyrCD1-CE2 was added to the force field. The partial charges of the modified tyrosines were corrected based on RESP charges obtained from HF/6-31G(d) calculations of a Tyr-Tyr system. The system was equilibrated just like in the w.t. protein.

### Migration free energy profiles

To study in detail the properties of the hydrophobic tunnels in trHbO from *M. tuberculosis*, we have calculated the migration free energy profiles for a diatomic neutral ligand along protein matrix identified tunnels, in both the oxy and deoxy proteins. The free energy profiles were constructed by performing constant velocity multiple-steered molecular dynamics (MSMD) simulations, and using the Jarzynski's inequality,<sup>24</sup> to compute the free energy.

Jarzynski's inequality relates the equilibrium free energy ( $\Delta A$ ) along the reaction coordinate with the irreversible work performed over the system when it is steered along the coordinate at constant temperature according to

$$\exp[-\Delta A(\xi)/k_B T] = \langle \exp[-W(\xi)/k_B T] \rangle$$

where  $W(\xi)$  is the external work performed on the system as it evolves from the initial to the final state along the reaction coordinate ( $\xi$ ), computed by integrating the force acting on the steering potential along  $\xi$ . The steering potential  $E(\xi)$  is a harmonic well that moves with constant velocity ( $v$ ) along the reaction coordinate

$$E(\xi) = k[\xi - (\xi_0 + v\Delta t)]^2$$

In this study, the reaction coordinate  $\xi$  was chosen as the iron-ligand distance. The force constant used was 200 kcal mol<sup>-1</sup> Å<sup>-1</sup>. The pulling velocities used were 0.025 Å/ps. This means that it is necessary to perform a 200 ps simulation to span a 5 Å distance.

To compute the free energy profile of ligand migration along a selected tunnel, we have performed at least 20 different MSMD simulations. We have divided them in

two blocks of 10 MSMD each to obtain two independent free energy profiles. The starting snapshots for each MSMD are taken from an equilibrated MD run with the ligand at fixed distance from the iron. The MSMD simulations were performed until the NO/O<sub>2</sub> molecule was completely solvated, close to the tunnel entry. Moving it further into the solution requires an additional expensive computational cost, because it becomes necessary to sample properly the solvent degrees of freedom. On the other hand, the MSMD simulations were started at 4 Å from the Fe atom, because, at shorter distances, it would be necessary to deal explicitly with a quantum description of the Fe-ligand chemical bond. The details of RC values for each case are given in the corresponding section.

This free energy calculation scheme has been successfully applied to compute the free energy profile of ligand migration in trHbN and also to compute free energies of enzymatic reactions.<sup>25,26</sup>

## RESULTS AND DISCUSSION

### Identification of possible migration tunnels

To explore the existence and location of possible tunnels for ligand migration in the deoxygenated structure of trHbO (trHbO-wt), we performed an initial set of 20 MSMD runs pulling the O<sub>2</sub> molecule of the active site. No other restriction but the Fe-O<sub>2</sub> distance (the selected reaction coordinate) was applied, thereby allowing O<sub>2</sub> to explore the best possible way out.

Visual inspection of the trajectories showed that there are two main paths for O<sub>2</sub> migration, following a long (~16 Å) and a short molecular tunnel (~10 Å) in the protein matrix, respectively (see Fig. 1). The long tunnel

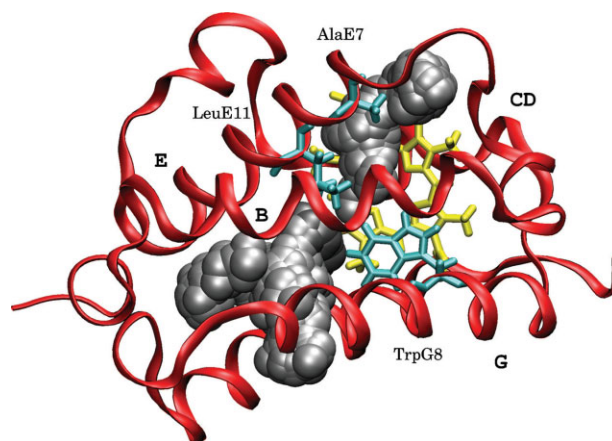


**Figure 1**

View of the long and short tunnel-E7 of trHbO. The heme group is shown in yellow, and the relevant residues are shown in light blue. Long and short tunnel is depicted in gray.

corresponds to that identified by Milani *et al.*<sup>20</sup> from an analysis of the protein crystal structure. In the same work, these authors proposed that a short tunnel, similar to the one detected in our simulations, could be operative for ligand migration; from its topological location, such path was reminiscent of the well-known distal gate “E7” ligand diffusion pathway of myoglobin. In the following, we will call the identified tunnels: “long tunnel,” and “short-tunnel E7,” respectively. In that work, the other short tunnel found in truncated hemoglobin N was discussed. However, as it will be shown later, in w.t. TrHbO, this tunnel seems to be blocked by TrpG8.

### Long tunnel of trHbO

As shown in Figure 1, the long tunnel is  $\sim 16$  Å long and connects the heme distal site with the solvent at a location between the B, E, and G helices. A detailed analysis of the MSMD runs allows identification of several structural characteristics of this tunnel. In the first place, the tunnel displays a very large cavity, similar to the secondary-docking sites identified in Mb and trHbN, in the region between 8 and 13 Å from the heme group. The cavity is defined by residues LeuE15, LeuH3, LeuH7, and MetG12. We found a small bifurcation near the exit of the tunnel, at  $\sim 16$  Å distance from the heme. We have observed that the distance between PheB2 and LeuH3 fluctuates widely along the simulation. When PheB2 and LeuH3 stay apart, the ligand may pass between them. However, when these residues stay close, the ligand is forced to follow a different path; thus, a diatomic ligand may leave the protein by using such tunnel bifurcation. Interestingly, our simulations show that the tunnel exhibits an interruption at a distance of  $\sim 6$  Å from the Fe atom due to clustering of the TrpG8, LeuE11, and MetG12 residues. These observations are consistent with the crystal structure analyses that showed that protein matrix tunnels are an immediately evident structural feature in group I trHbs,<sup>27,28</sup> whereas in the static structures of trHbOs identification of a continuous long tunnel path is more complex.<sup>7,20</sup>

### Thermodynamic characterization of the migration along the tunnels

By using Jarzinski's inequality, our method allows to obtain free energy profiles associated with the oxygen migration process. The free energy profile associated to the long tunnel is shown in Figure 2(a). The profile shows a deep and wide minimum between 8 and 11 Å distance from the heme, corresponding to the ligand-docking site described previously.<sup>20</sup> The figure also shows that two different pathways may exist in the range between 11 and 16 Å for the long tunnel, consistently with the results observed in Figure 1. The barrier heights are similar in both branches. Finally, a significant barrier

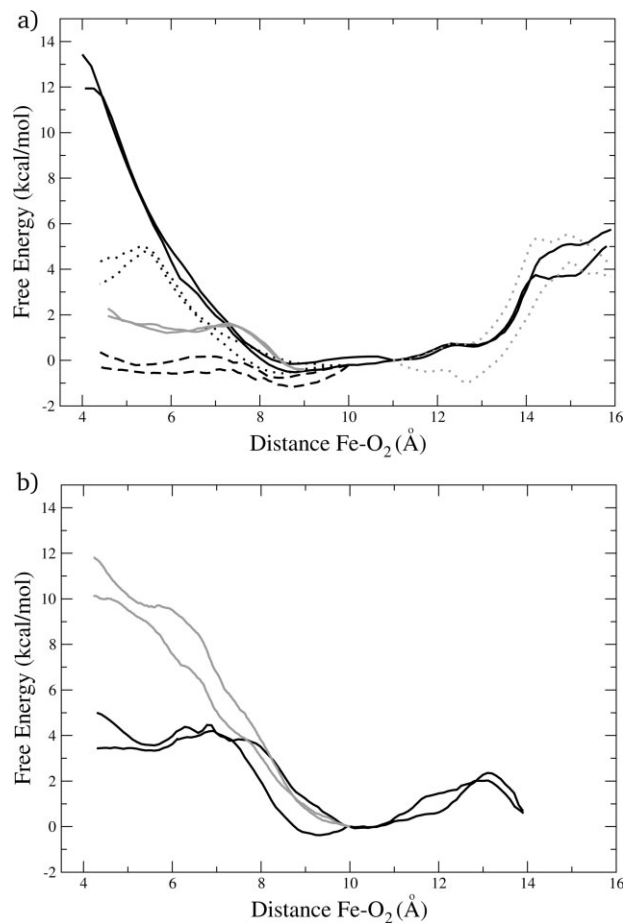


**Figure 2**

(a) Free energy profiles for ligand migration through long tunnel in trHbO-wt, trHbOWG8F, and trHbOWG8A depicted in black solid, black dotted, and gray solid lines, respectively. The alternative path for ligand exits at the end of the tunnel in dotted gray. The profile corresponding to the tunnel-G8 in the trHbOWG8A is shown in dashed gray solid line. (b) Free energy profiles for ligand migration through the short tunnel-E7. Results for w.t. and trHbOAE7I are depicted in black and gray, respectively. For each case, two independent free energy profiles are shown.

(between 6 and 4 Å from the heme) that the ligand must cross to access the heme-Fe atom is observed.

### Mutant proteins TrpG8 → Phe (trHbOWG8F) and TrpG8 → Ala (trHbOWG8A)

To assess the role of TrpG8 in building the free energy barrier found at 4–6 Å from the heme, we constructed *in silico* two mutants in which TrpG8 was replaced by Phe and Ala, respectively. We present in Figure 2(a) the free energy profile for both mutant proteins. As expected, the barrier for ligand migration is dramatically decreased from 12 to 5 kcal/mol, and to only 2 kcal/mol, in the cases of the Phe and Ala mutants, respectively. This confirms our hypothesis that TrpG8 is the key residue involved in restricting ligand diffusion through the long



tunnel. Interestingly, TrpG8 is a conserved residue throughout trHb groups II and III, while it is strictly absent in group I, hosting *M. tuberculosis* trHbN, where it is replaced by Val. New experimental evidence indicates that the mutant protein trHbOWG8F has a kinetic constant ( $k_{\text{on}}$ ) a little bigger than w.t. protein ( $k_{\text{onO}_2\text{-wt}}$ ,  $1.1\text{--}8.5 \times 10^5 \text{ M}^{-1} \text{ s}^{-1}$ ;  $k_{\text{onO}_2\text{-WG8F}}$ ,  $1.27 \times 10^6 \text{ M}^{-1} \text{ s}^{-1}$ ).<sup>29</sup>

The replacement of Trp by Ala produces a decrease in the migration barrier along the long tunnel. We noticed that, in this case, a new and different short tunnel appears in the direction of the G8 site, which was originally blocked by Trp. This new short tunnel, which we will call short-tunnel G8 for simplicity, connects the iron atom and the distal heme cavity with the solvent, pointing in a direction opposite to the E7 residue (see Fig. 3). The free energy profile for the short-tunnel G8, obtained through MSMD simulations, presents a barrier to ligand diffusion lower than 2 kcal/mol [Fig. 2(a)]. It is interesting to note that this tunnel corresponds to the short-tunnel branch of trHbN, postulated to be the principal O<sub>2</sub> migration path in the deoxy protein.<sup>25</sup>

### The short-tunnel E7

As mentioned earlier, w.t. trHbO displays a second tunnel for ligand migration, identified earlier as a short-tunnel E7 (see Fig. 1). This tunnel has been already identified by Milani *et al.*<sup>4</sup> and is topologically related to the ligand distal entry pathway of myoglobin (Mb), extending through the HisE7 gate, as originally proposed by Perutz *et al.*<sup>5</sup> The relevant trHbO residues along this tunnel are AlaE7, TyrB10 and TyrCD1, and the heme propionate group. The free energy profile for this tunnel, shown in Figure 2(b), indicates that the barrier for ligand entry along the tunnel is 4 kcal/mol. This value is smaller than that found for the long tunnel discussed earlier, suggesting that in the w.t. protein ligand migration will probably occur through the tunnel-E7 pathway.

### trHbO mutation at the E7 site

To confirm the role of the distal residue AlaE7 in promoting ligand migration through the proposed short-tunnel E7, we examined the trHbO mutant bearing the AlaE7 → Ile replacement (trHbOAE7I). The aim of such mutation is to block the tunnel with a bulkier residue, which should display a higher barrier to ligand migration. The corresponding profile shows, as expected, a higher barrier relative to that of the w.t. protein [Fig. 2(b)]. This clearly shows the relevance of the size of the E7 residue for ligand migration in trHbO, as shown by experimental approaches on E7 Mb mutants.<sup>30</sup> These results suggest that trHbO mutants bearing bulky E7 residues should present lower ligand association rates constants.

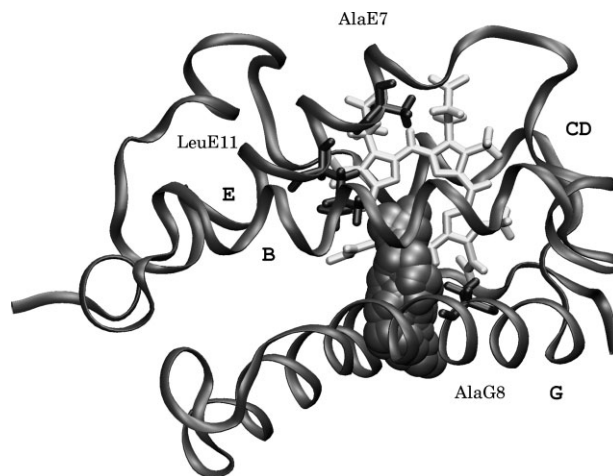


**Figure 3**

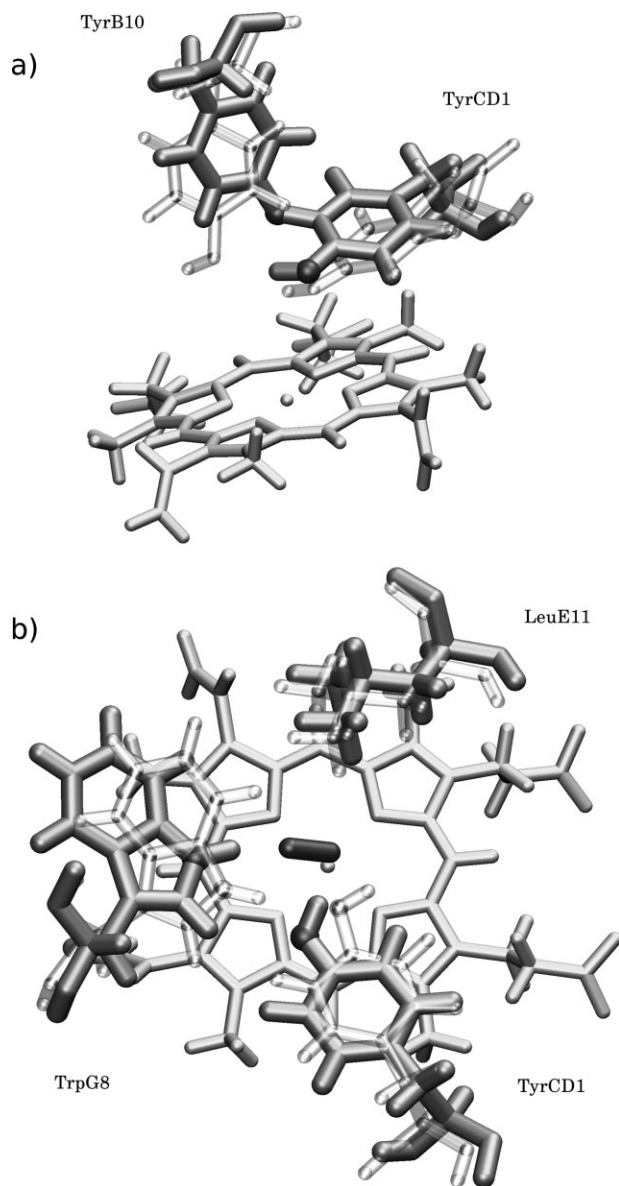
View of the trHbOWG8A. The sites explored by an O<sub>2</sub> probe molecule along the short tunnel-G8 are shown.

### Role of the TyrB10-TyrCD1 intramolecular covalent bond

As already mentioned, the X-ray structure of trHbO shows an unusual covalent bond between TyrB10 and TyrCD1 for half of the molecules in the crystallized dodecamer [Fig. 4(a)]. In this section, we present results concerning the influence of this bond on the ligand migration free energy profiles. Although the position of this bond seems to affect only ligand migration through the short-tunnel E7, we calculated the profiles associated to both tunnels. Figure 5(a) shows the free energy profiles for ligand migration through the tunnels in the presence of the covalent Tyr—Tyr bond (trHbO-wtTyrTyr). For both tunnels, the profiles are similar to those of trHbO free of the Tyr—Tyr bond, but in the long tunnel the shape of the profiles are different. In trHbO-wtTyrTyr, a shoulder at 9 Å of the iron atom appears. This is probably related to rotation of LeuH7 that stay closer to LeuE15 when the protein hosts the Tyr—Tyr bond.

### Role of the tunnel/cavity system in multiligand chemistry

Once the oxygen is bound to the Fe atom, a second ligand (i.e., NO) could migrate into the heme distal site of the oxygenated trHbO (trHbO-wtOxy) and react to yield nitrate. In trHbN, it was found that subtle alterations in the protein dynamics of the oxygenated protein results in different migration paths.<sup>25</sup> To analyze whether such a mechanism is also operative in trHbO, we computed the corresponding free energy profiles for the long and short tunnels E7 for the oxygenated protein. Figure 5(b) shows the free energy profile corresponding to migration of NO into the protein for the long- and

**Figure 4**

(a) Schematic representation of the neighboring location of trHbO-wtTyrTyr distal site, showing the covalently linked TyrB10-TyrCD1 pair. The lighter color reflects the arrangement of the residues without the covalent bond TyrTyr. (b) Schematic representation of the heme distal sites of trHbO-wt and trHbO-wtOxy. The heme group, TrpG8, and LeuE11 are shown. The lighter color reflects the arrangement of the residues before O<sub>2</sub> binding.

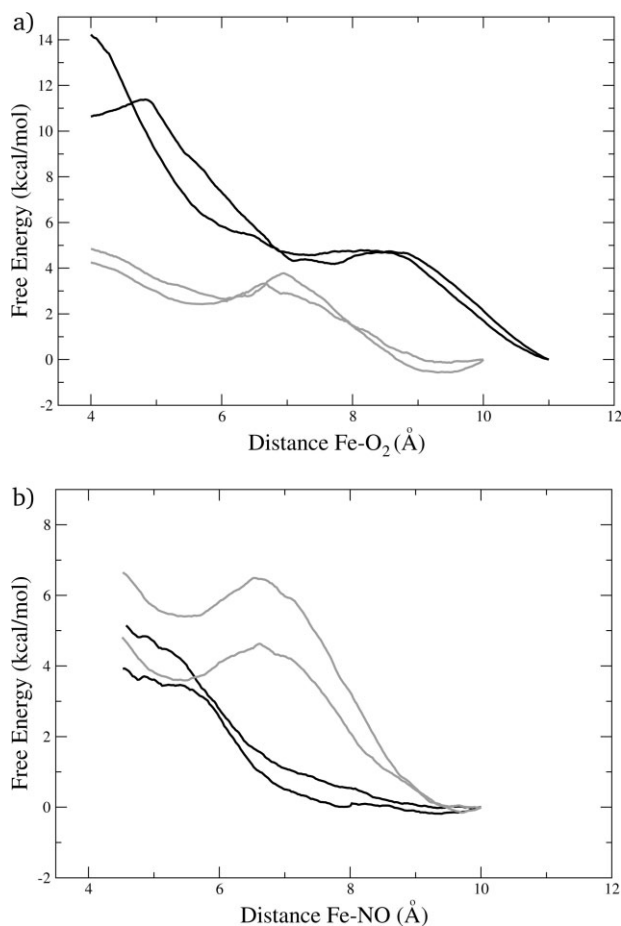
short-tunnel E7. Our results show that in the long tunnel the barrier is significantly reduced from 12 kcal/mol in the deoxygenated protein to 4 kcal/mol in oxygenated trHbO. On the other hand, the barrier for ligand migration, corresponding to the short tunnel, is similar in both the oxygenated and deoxygenated proteins.

It is important to note that when comparing the oxy and deoxy states, although the short-tunnel E7 barrier has the

same height, it is located at different values of the reaction coordinate, evidencing that the active site undergoes some change upon oxygenation

The simulation results suggest that modulation of the free energy barrier for ligand migration through the long tunnel is achieved via the displacement of TrpG8 following O<sub>2</sub> binding. As shown in Figure 4(b), when O<sub>2</sub> is coordinated to the heme-Fe atom, TrpG8 moves away from LeuE11 to form a hydrogen bond with the distal oxygen molecule. This displacement results in reduced steric hindrance for diatomic ligand migration to the heme, and in a concomitant decrease of the diffusion-free energy barrier. The results are consistent with the previously observed data from UV-enhanced resonance Raman spectroscopy, which indicate a significant conformational change in the G8 tryptophan with ligation.<sup>16</sup>

Taken together, the results from oxygenated and deoxygenated trHbO suggest that the effective barrier for

**Figure 5**

(a) Free energy profiles in trHbO-wtTyrTyr long and short E7 tunnels depicted in black and gray lines, respectively. (b) Free energy profiles in trHbO-wtOxy long and short E7 tunnels. In both cases, only the profile between 4 and 10 Å is shown. For each case, two independent free energy profiles are shown.

ligand migration of the second ligand to the distal site is similar to the barrier met by first ligand. However, while in the deoxygenated case, the (first) ligand would migrate through the short-tunnel E7; in the oxygenated case, the (second) ligand can migrate through both the long-channel and the short-tunnel E7, encountering similar barriers. These data are consistent with the experimental data, because the oxygen association  $k_{\text{onO}_2}$  and NO oxidation  $k_{\text{oxNO}}$  rate constants are very similar, of  $1.1\text{--}8.5 \times 10^5 \text{ M}^{-1} \text{ s}^{-1}$  and  $6.0 \times 10^5 \text{ M}^{-1} \text{ s}^{-1}$ , respectively.<sup>4</sup>

## DISCUSSION

We have analyzed the ligand migration process in w.t. and in single-site mutants of *M. tuberculosis* trHbO. Using a MSMD scheme and Jarzinski's inequality, we have computed the free energy profiles for ligand migration along the tunnels that connect the protein heme distal site to the bulk solvent. The free energy barrier that the ligand (diffusing along the explored paths) must overcome to access the active site is the main determinant for the ligand-association rates.

Our results show that, in w.t. trHbO, the ligands migrate likely through the short-tunnel E7, meeting a barrier whose height is  $4 \pm 1$  kcal/mol. However, once the protein is oxygenated, both tunnels can contribute to ligand entry, because they present similar barriers. This mechanism is different from the case of trHbN, in which each ligand migrate through a different pathway.<sup>25</sup> The change in the free energy barrier from the long tunnel is due to the TrpG8 interaction with the heme-bound  $\text{O}_2$ . The short-tunnel E7 barrier does not change significantly upon oxygenation; consequently, the overall barrier presented by the short-tunnel E7 is similar in the oxygenated and deoxygenated states of the protein. This fact is consistent with the experimental kinetic constants for ligand migration.

The study of the single-site mutants allows understanding the role played by TrpG8, AlaE7, and TyrCD1 in controlling the accessibility to the heme. The results highlight the trHbOWG8A mutant as the relevant species to be investigated experimentally, because it should exhibit association rate constants ( $k_{\text{on}}$ ) higher than those of w.t. trHbO. Most notably, the double-mutant trHbOWG8A-AE7I should completely alter the ligand-binding pattern, with a closed short tunnel, an accessible long tunnel, and a new accessible pathway (G8 pathway).

TrHbO, displaying the TyrCD1-TyrB10 covalent bond, shows some differences (compared to the protein free of such intermolecular cross-link) in the profiles for ligand migration through the long tunnel but not in the short tunnel. In the long tunnel, although the barrier is not changed, a shoulder appears at about 9 Å. The shoulder arises from rotation of LeuH7, which now blocks the tunnel partially.

Finally, the most intriguing point, derived from our results, is the critical role played by TrpG8 in trHbO ligand migration and binding characteristics. This consideration seems even more important if we take into account that TrpG8 is totally conserved in all group II and III trHbs sequenced to date. It has been found that TrpG8 is not only responsible for the high barrier observed in the long tunnel, but it also blocks the short tunnel branch displayed by group I trHbs. Moreover, our results for the oxy protein show that TrpG8 also interacts with the coordinated oxygen. This indicates that the presence of the conserved residues in group II and group III but not group I, is responsible for the significantly different migration patterns in trHbO and trHbN. All these data suggest that experiments on TrpG8 mutants should be given first priority for shedding light on the structure to function relationship in trHbOs, but also in group III trHbs.

## ACKNOWLEDGMENTS

M.B. is grateful to CIMAINA (University of Milano) for continuous support. F.J.L. acknowledges Barcelona Supercomputer Center for providing access to the Marenostrum supercomputer.

## REFERENCES

- Collins FM. Tuberculosis: the return of an old enemy. *Crit Rev Microbiol* 1993;19:1–16.
- Kochi A. The global tuberculosis situation and the new control strategy of the World Health Organization. *Tubercle* 1991;72:1–6.
- Sudre P, Ten Dam G, Kochi A. Tuberculosis: a global overview of the situation today. *Bull World Health Org* 1992;70:149–159.
- Milani M, Pesce A, Nardini M, Ouellet H, Ouellet Y, Dewilde S, Bocedi A, Ascenzi P, Guertin M, Moens L, Friedman JM, Wittenberg JB, Bolognesi M. Structural bases for heme binding and diatomic ligand recognition in truncated hemoglobins. *J Inorg Biochem* 2005;99:97–109.
- Perutz MF, Fermi G, Luisi B, Shaanan B, Liddington RC. Stereochemistry of cooperative mechanisms in hemoglobin. *Acc Chem Res* 1987;20:309–321.
- Bolognesi M, Bordo D, Rizzi M, Tarricone C, Ascenzi P. Nonvertebrate hemoglobins: structural bases for reactivity. *Prog Biophys Mol Biol* 1997;68:29–68.
- Nardini M, Pesce A, Milani M, Bolognesi M. Protein fold and structure in the truncated (2/2) globin family. *Gene* 2007;398:2–11.
- Ouellet H, Ouellet Y, Richard C, Labarre M, Wittenberg B, Wittenberg J, Guertin M. Truncated hemoglobin HbN protects *Mycobacterium bovis* from nitric oxide. *Proc Natl Acad Sci USA* 2002;99:5902–5907.
- Giordano R, Teixeira J, Wanderlingh U. Dynamics of water on protein surfaces. *Phys B Condens Mater* 1995;213–214:769–771.
- Bonamore A, Attili A, Arengi F, Catacchio B, Chiancone E, Morea V, Boffi A. A novel chimera: the “truncated hemoglobin-antibiotic monooxygenase” from *Streptomyces avermitilis*. *Gene* 2007;398:52–61.
- Vuletic DA, Lecomte JT. A phylogenetic and structural analysis of truncated hemoglobins. *J Mol Evol* 2006;62:196–210.
- Colasanti M, Gradoni L, Mattu M, Persichini T, Salvati L, Venturini G, Ascenzi P. Molecular bases for the anti-parasitic effect of NO (Review). *Int J Mol Med* 2002;9:131–134.
- Ascenzi P, Salvati L, Bolognesi M, Colasanti M, Polticelli F, Venturini G. Inhibition of cysteine protease activity by NO-donors. *Curr Protein Pept Sci* 2001;2:137–153.

14. Crespo A, Marti MA, Kalko SG, Morreale A, Orozco M, Gelpi JL, Luque FJ, Estrin DA. Theoretical study of the truncated hemoglobin HbN: exploring the molecular basis of the NO detoxification mechanism. *J Am Chem Soc* 2005;127:4433–4444.
15. Fabozzi G, Ascenzi P, Renzi SD, Visca P. Truncated hemoglobin GlnO from mycobacterium leprae alleviates nitric oxide toxicity. *Microb Pathog* 2006;40:211–220.
16. Ouellet H, Juszczak L, Dantsker D, Samuni U, Ouellet YH, Savard PY, Wittenberg JB, Wittenberg BA, Friedman JM, Guertin M. Reactions of mycobacterium tuberculosis truncated hemoglobin O with ligands reveal a novel ligand-inclusive hydrogen bond network. *Biochemistry* 2003;42:5764–5774.
17. Pathania R, Navani NK, Rajamohan G, Dikshit KL. Mycobacterium tuberculosis hemoglobin Hbo associates with membranes and stimulates cellular respiration of recombinant *Escherichia coli*. *J Biol Chem* 2002;277:15293–15302.
18. Liu CHY, Chang Z. Truncated hemoglobin O of mycobacterium tuberculosis: the oligomeric state change and the interaction with membrane components. *Biochem Biophys Res Commun* 2004;316:1163–1172.
19. Ouellet H, Rangelova K, LaBarre M, Wittenberg JB, Wittenberg BA, Magliozzo RS, Guertin M. Reaction of mycobacterium tuberculosis truncated hemoglobin O with hydrogen peroxide: evidence for peroxidatic activity and formation of protein-based radicals. *J Biol Chem* 2007;282:7491–7503.
20. Milani M, Savard PY, Ouellet H, Ascenzi P, Guertin M, Bolognesi M. A TyrCD1/TrpG8 hydrogen bond network and a TyrB10-TyrCD1 covalent link shape the heme distal site of mycobacterium tuberculosis hemoglobin O. *Proc Natl Acad Sci USA* 2003;100:5766–5771.
21. Jorgensen WL, Chandrasekhar J, Madura JD, Impey RW, Klein ML. Comparison of simple potential functions for simulating liquid water. *J Chem Phys* 1983;79:926–935.
22. Ryckaert JP, Ciccoti G, Berendsen HJC. Numerical integration of the cartesian equations of motion of a system with constraints: molecular dynamics of n-alkanes. *J Comput Phys* 1977;23:327–341.
23. Pearlman DA, Case DA, Caldwell JW, Ross WS, Cheatham Iii TE, DeBolt S, Ferguson D, Seibel G, Kollman P. AMBER, a package of computer programs for applying molecular mechanics, normal mode analysis, molecular dynamics and free energy calculations to simulate the structural and energetic properties of molecules. *Comput Phys Commun* 1995;91:1–41.
24. Jarzynski C. Nonequilibrium equality for free energy differences. *Phys Rev Lett* 1997;78:2690–2693.
25. Bidon-Chanal A, Marti MA, Crespo A, Milani M, Orozco M, Bolognesi M, Luque FJ, Estrin DA. Ligand-induced dynamical regulation of NO conversion in mycobacterium tuberculosis truncated hemoglobin-N. *Proteins Struct Funct Bioinf* 2006;64:457–464.
26. Crespo A, Marti MA, Estrin DA, Roitberg AE. Multiple-steering QM-MM calculation of the free energy profile in chorismate mutase. *J Am Chem Soc* 2005;127:6940–6941.
27. Milani M, Pesce A, Ouellet Y, Ascenzi P, Guertin M, Bolognesi M. Mycobacterium tuberculosis hemoglobin N displays a protein tunnel suited for O<sub>2</sub> diffusion to the heme. *EMBO J* 2001;20:3902–3909.
28. Milani M, Pesce A, Ouellet Y, Dewilde S, Friedman J, Ascenzi P, Guertin M, Bolognesi M. Heme-ligand tunneling in group I truncated hemoglobins. *J Biol Chem* 2004;279:21520–21525.
29. Ouellet H, Milani M, LaBarre M, Bolognesi M, Couture M, Guertin M. The roles of Tyr(CD1) and Trp(G8) in mycobacterium tuberculosis truncated hemoglobin O in ligand binding and on the heme distal site architecture. *Biochemistry* 2007;46:11440–11450.
30. Eich RF, Li T, Lemon DD, Doherty DH, Curry SR, Aitken JF, Mathews AJ, Johnson KA, Smith RD, Phillips GN, Jr, Olson JS. Mechanism of NO-induced oxidation of myoglobin and hemoglobin. *Biochemistry* 1996;35:6976–6983.